IJBPAS, November, 2022, 11(11): 5267-5285

ISSN: 2277–4998

International Journal of Biology, Pharmacy and Allied Sciences (IJBPAS)

'A Bridge Between Laboratory and Reader'

www.ijbpas.com

IDENTIFICATION OF POTENTIAL DRUG CANDIDATES FOR B-CELL LYMPHOMAS BY USING STRUCTURAL ANALOGUES OF PANOBINOSTAT BY MOLECULAR DOCKING STUDIES WITH BCL-6 GENE

CHINARI SK[1], MITTAL S[2] AND CHITRA V[1*]

1: Master of Pharmacy, Department of Pharmacology, SRM College of Pharmacy, SRMIST, Kattankulathur-603203, Tamil Nadu, India

2: Master of Pharmacy, Department of Pharmaceutics, Delhi Institute of Pharmaceutical Sciences and Research, DPSRU, New Delhi-110017, New Delhi, India

3: PhD, Department of Pharmacology, SRM College of Pharmacy, SRMIST, Kattankulathur-603203, Tamil Nadu, India

***Corresponding Author: Dr. Vellapandian Chitra: E Mail: chitrav@srmist.edu.in**

Received 26th Dec. 2021; Revised 24th Jan. 2022; Accepted 14th Feb. 2022; Available online 1st Nov. 2022

https://doi.org/10.31032/IJBPAS/2022/11.11.6572

ABSTRACT

Objective: To identify a potential drug molecule for B-cell lymphoma based on the structural analogues of Panobinostat, a Histone Deacetylase Inhibitor via in silico docking studies against the BCL6 gene and compared with Panobinostat.

Materials and Methodology: BCL6 protein structure was downloaded from the RCSB protein databank. The ligands were selected and downloaded from PubChem. The docking study was carried out using Flare docking software. The pharmacokinetic studies were done using the SwissADME web tool.

Results: The in silico studies identified molecules with better binding energy than Panobinostat(-7.507 Kcal/mol). The top 5 molecules were studied for their interaction with the gene having a range of binding energy from -10.339 to -9.935 kcal/mol. The rank of the compounds was determined based on the lowest energy score.

Conclusion: The docking study data and pharmacokinetic data suggested that the molecule named CHEMBL341601 (PubChem ID: 11058122) could be used as a potential drug for Lymphoma.

Keywords: In-silico docking study, Panobinostat, B-Cell Lymphoma, Histone Deacetylase Inhibitor, BCL6 gene, Flare by Cresset

1. INTRODUCTION

Lymphoma, a rare form of cancer, has affected around 627,439 people in 2020 **[1]**. It involves the malignancy of the lymphatic system that is caused due to the clonal proliferation of B-Cells, T-cells, and Natural Killer cell subsets of lymphocyts at various stages of maturation **[2]**. Body's lymphatic system is a natural germ-fighting defence mechanism that comprises various organs like lymph nodes/glands, spleen, thymus gland and the bone marrow. Broadly, Hodgkin's Lymphoma (HL) and Non-Hodgkin's Lymphoma (NHL) are the two major types of lymphomas, which comprise of majority of the lymphomas **[3]**. The NHL is further classified into subtypes depending upon the type of cells they affect, which include B-cells, T-cells, and Natural Killer (NK) cells. Some of those lymphomas include **[4]**

1. Diffused Large B Cell Lymphoma (DLBCL)
2. Lymphoplasmacytic lymphoma
3. Primary Mediastinal Large B-Cell Lymphoma (PM-LBCL)
4. Intravascular Large B-Cell Lymphoma (I-LBCL)
5. ALK+ large B-cell lymphoma
6. T-cell/histiocyte-rich large B-cell lymphoma
7. T-cell prolymphocytic leukaemia
8. Aggressive NK-cell leukaemia
9. Enteropathy-associated T-cell lymphoma
10. Primary cutaneous CD30+ T-cell lymphoproliferative disorder

Diffused large B cell lymphoma (DLBCL) is considered one of the most prevalent forms of non-Hodgkin's Lymphoma **[5]**. It accounts for 30% of all the NHL cases **[6]**. Generally, it is presented with a rapidly growing mass or as an enlarged lymph node. B cell lymphomas are a result of the malignant proliferation of the B cell during the different stages of their development. There are three stages of development, pre-germinal, germinal, and post-germinal centre, of which most of the lymphomas are derived from the germinal centre (GC) **[7]**.

B cell Lymphoma (BCL) gene is a family of genes that is responsible for the regulation of different BCL proteins that act as a transcription repressor and have significance in Lymphomas. The BCL 6 is a part of the BTB/POZ zinc finger family of the transcription repressor, which

expresses itself during the GC differentiation phase **[8]**. The presence of BCL6 is essential for the formation of GCs and the further differentiation of B-cells into memory cells or plasma cells by its downregulation **[9]**. Around 20% to 40% of the cases of DLBCL have shown BCL6 gene alterations **[7]**. These genetic alterations usually involve translocations that fuse with the coding sequence of the homologues promoters, otherwise, it could be due to a point mutation in the BCL 6 promoter negative regulatory element **[10]**. As GCs cannot form in the absence of BCL 6, it indicates that BCL 6 facilitates the proliferative and genetically unstable centroblast phenotype, alongside BCL 6 has shown to weaken the DNA damage sensing **[11]**. The B cells become centroblasts after they enter the GC reaction that causes them to gain the ability to divide and multiply at a high rate and at the same time experience immunoglobulin somatic hypermutation (SHM) which is controlled by activation-induced cytosine deaminase (AID) **[12]**. Functional gain and loss studies of the DLBCL showed BCL 6 damaged the histone 2x phosphorylation and double-strand break repair once it was exposed to DNA damaging agent **[11]**. The BCL 6 enables the down streaming of the checkpoint genes of ATR inducing TP53 **[13]**, CHEK1 **[14]** and CDKN1A **[15]**.

The BCL6 gene is known to be associated with Primary Mediastinal Large B-Cell Lymphoma (PMLBCL) **[16]**. PMLBCL is a type of aggressive DLBCL, but WHO classifies it separately, mainly due to the specific clinical and pathological features. The Primary Mediastinal LBCL is seen in around 2-4% of all NHL and around 6% of DLCBL. It primarily affects young adults of age around 35 years, widely females **[17]**. Some studies have shown the somatic hypermutation of the BCL6 gene and immunoglobulin gene in PMLBCL. This has confirmed the post-germinal centre of origin for the cancerous cells **[18]**.

Two 2003 studies have shown that the molecular transcriptional pattern of PMLBCL was unique and different from DLBCL, although it has shared features with classical Hodgkin Lymphoma (cHL) **[19][20]**.

The drug molecule, Panobinostat was selected for the study due to its novel approach as chemotherapeutic agent and due to its current investigations for treatment of multiple types of cancers. Panobinostat (tradename Farydak) is a small molecule oral drug which acts as a Histone Deacetylase Inhibitor (HDAC). It was approved by the US FDA (US Food and Drug Agency) on 15th February 2015 as an antineoplastic agent for the treatment of Multiple Myeloma in combination with Bortezomib and dexamethasone **[21][22]**.

Subsequently, the EMA (European Medicines Agency granted approval on 15th August 2015 for the same indication **[23]**. The activity of Panobinostat is based on the deacetylase enzyme that is also known as HDACs proteins, which primarily acts on the histone proteins along with the transcription factors. The arrangement of the DNA into nucleosomes are done by histone proteins. During the cell division process, the HDACs proteins execute the histone modification which drives towards the different conformations of chromatin, allowing the DNA transcription **[24]**. Together with histone acetyltransferases with their contrasting activities, they regulate various cellular activities including cell differentiation, gene expression and survival **[25-27]**. There are four main classes of HDACS (I, II, III, and IV) that are relocated from the cytoplasm into the nucleus and primarily act on non-histone proteins. The drug panobinostat has shown activity in four classes during preclinical studies **[28]**. HDAC inhibitors like panobinostat cause an elevation in the acetylation process leading to the increase of DNA transcription and accumulation of other proteins. This leads to a reduction in cellular proliferation and further apoptosis **[29]**.

At present, various clinical trials are being conducted for various diseases other than Multiple Myeloma. These include relapsed DLBCL, non-small cell lung cancer, and breast cancer, with or without in combination with rituximab, erlotinib and letrozole **[30-33]**. The drug description of Panobinostat is provided in **Table 1**.

2. MATERIALS AND METHODOLOGY

2.1.Target Protein Acquisition and Preparation.

A three-dimensional structure of the BCL 6 gene was obtained from the RCSB Protein DataBase for the docking study in the PDB format **[34]**. The target gene's PDB ID was 6WE6 which was a Camphor bound P450cam D251E structure **[35]**. The target's structure was determined using the X-ray diffraction method. Protein preparation was carried out in Flare docking software, developed by Cresset group **[36]** using the default settings.

2.2.Ligand Preparation

The drug of interest was selected to be Panobinostat, which is an oral Histone Deacetylase inhibitor. The three-dimensional molecular conformers of the compound were obtained from PubChem **[37]**. A library of compounds was compiled by searching for the compounds with structural similarity. A total of 88 compounds including Panobinostat was selected and downloaded in SDF format. The two-dimensional structure of the selected ligands is available in **Table 2**.

The ligand structure was prepared by using the default preparation wizard in Flare software (Cresset module) **[36]**. The ligand files were read in autodetect mode at full protonation.

2.3.Molecular Docking Studies

Molecular docking of all 88 selected compounds including Panobinostat listed in the ligand library with the BCL 6 gene was carried out using Flare module by CRESSET software **[36]**. The grid box was defined using binding site information in normal mode and docking calculation was done in the CRESSET Flare module with default settings. The top 5 compounds with the lowest LF Rank scores were selected and their best poses were generated and visualised.

3. RESULTS AND DISCUSSION

Molecular docking of the selected 88 compounds was carried out on the B-Cell Lymphoma 6 (PDB ID:6WE6) gene in CRESST Flare software for the identification of the interactions between the target protein and the ligands. The CRESSET Flare software uses the polarisable extension electron distribution (XED) force field as the docking protocol **[38]**. The 3D crystal structure of the gene was downloaded from the PDB databank. The structure of panobinostat and the structural analogues were downloaded from PubChem in SDF format.

The binding affinities of the ligands towards the BCL6 gene were studied in detail. Various interactions between the ligand and protein were identified. LF rank score is a measure of the binding affinity of the protein-ligand complex. The list of LF rank scores of all the ligands is given in **Table 2**. A higher negative LF score indicates a better affinity towards the BCL6 gene. All the molecules selected for the docking studies showed binding affinity towards the gene. The LF rank score ranged from a value of -10.339 kcal/mol to -3.052 kcal/mol. The docking results showed that some of the molecules that have structural similarity with Panobinostat had better docking to the target protein, BCL-6 when compared to Panobinostat. The LF rank score of Panobinostat was calculated to be -7.507 kcal/mol. Panobinostat had 3 interactions in total with 1 C-O covalent bond and 2 hydrogen bonds at Cys 53, Cys 53, and Glu 115 amino acid residues with bond lengths of 2.8 Å, 2.5 Å and 2.6 Å **(Figure 1a)**. On the other hand, a molecule named CHEMBL3793310 (IUPAC Name: (E)-N-Hydroxy-3-[4-[2-[(E)-2-(2-methyl-1H-indol-3-yl)ethenyl]phenyl]phenyl]prop-2-enamide) (PubChem ID: 127030313) showed the highest binding affinity with an LF Rank score of -10.339 kcal/mol **(Figure 1b)**. The other four ligands had an LF rank score of -10.233, -10.077, -10.071 and –9.935 kcal/mol, respectively. The best

poses of the top 5 molecules along with Panobinostat against the active site of the BCL6 gene were captured for detailed studies. The details of the top 5 ligands including binding affinity, interactions, amino acid residues, and bond length have been given in **Table 2**.

The docking results revealed that all top 5 molecules with the lowest LF rank scores had one aromatic interaction with the BCL6 gene at the amino acid residue Tyr 58 of chain A. CHEMBL3793310 (PubChem ID: 127030313) with an LF rank score of -10.339 kcal/mol had 3 interactions that included a hydrogen bond, a C-O covalent bond and a pi-pi interaction. The bond lengths of the interactions were 2.8 Å, 2.8 Å, and 4.9 Å at amino acid residues Met 51, Met 51, and Tyr 58, respectively. CHEMBL341601 (PubChem ID: 11058122) with an LF rank score of -10.233 kcal/mol had 6 interactions with bond lengths of 3.0 Å, 2.8 Å, 2.8 Å, 2.4 Å, 3.0 Å, and 3.5 Å at Cys 53, Glu 114, Gln 133, Gln 133, Met 51 and Tyr 58 respectively **(Figure 1c)**. CHEMBL1819255 (Pubmed ID: 20579392) with LF rank score -10.077 kcal/mol had only 2 interactions, one hydrogen bond and the other pi-pi interaction **(Figure 1d)**. 3-(4-(di(1H-indol-3-yl)methyl)phenyl)-N-hydroxyacrylamide (PubChem ID: 11993595) with LF rank score of -10.071 kcal/mol showed 4 interactions including one O=O double bond **(Figure 1e)**. The bond lengths of interactions were 2.0 Å, 2.9 Å, 2.8 Å, and 3.2 Å at Glu 115, Met 114, Gln 113, and Tyr 58. The final compound with an LF rank score of -9.935 kcal/mol was CHEMBL1093052 (PubChem ID: 46197795) with 3 interactions. Bond lengths were 2.9 Å at Met 51, Glu 115, and 5.0 Å Tyr 58 **(Figure 1f)**.

3.1.In Silico Prediction of Drug Likeliness

One of the most significant criteria of prediction of drug likeliness is Lipinski's rule of 5, where if a chemical compound exhibits some biological activity and has physicochemical properties, would potentially make it an orally active drug molecule **[39]**. It uses various descriptors that are necessary for the prediction. The rules state

1. The molecular mass of less than 500 Daltons
2. Maximum 5 Hydrogen bond donors
3. Maximum 10 Hydrogen bond acceptors
4. Partition coefficient (Log_P) value not greater than 5

In case there are more than 3 violations of the descriptor parameters, then the compound is a misfit for the criteria of drug likeliness and is removed from the drug discovery process.

Egan's rule was developed as a model to predict bioavailbility based on LogP and Polar Surface Area (PSA) values **[40]**. Thus a molecule is deemed to have a good bioavailability when

1. Partition Coefficient (LogP) value is smaller or equal to 5.88
2. Polar surface area is lesser or equal to 131.6. Å

The Muegge's method involves use of more parameters for assessing the bioavailability of a molecule [41]. These parameters include

1. Molecular mass range from 200 to 600 Daltons
2. Partition coefficient (LogP) value between -2 to 5
3. Number of rings less or equal to 7
4. More than 4 carbon atoms
5. More than 1 heteroatom
6. Polar surface area less or equal to 150 Å
7. Rotatable bonds less or equal to 15
8. Hydrogen bond acceptors less or equal to 10
9. Hydrogen bond donors less or equal to 5

The Ghose filter provides an analysis of some computational physicochemical properties and the chemical constitutes of the known drug molecules that are readily available in the Comprehensive Medicinal Chemistry database **[42]**. The rule states that

1. Partition coefficient (LogP) value between -0.4 to 5.6 (mean value 2.3)
2. Molecular weight between 160 to 480 Daltons
3. Molecular refractivity between 40 to 130 (mean 97)
4. Number of atoms between 20 and 70
5. Polar surface area less than 150 Å

Finally, the Veber's rule states that **[43]**

1. Rotatable bonds less or equal to 10
2. Polar surface area less or equal to 140 Å

Table 3 provides the drug likeliness using various rules including Lipinski rule of 5, Veber, Ghose, Muegge, and Egan rules that were applied to the selected molecules. It was observed that none of the molecules violated Lipinski's rule of 5, while there were only a few that violated the other rules. All of these compounds show a low value of synthetic accessibility, thus indicating that they can be synthesised.

3.2.In Silico Simulations of Pharmacokinetics Properties

All 88 selected compounds including Panobinostat are screened for their pharmacokinetic properties using the online web tool SwissADME. The list of the findings has been given in the table, The pharmacokinetic data showed that of the top 5 molecules with the lowest LF Rank score, all of them had high GastroIntestinal

(GI) absorption, while only CHEMBL341601 (PubChem ID: 11058122) could cross the Blood-Brain Barrier (BBB). Moreover, only one compound of the top 5 molecules, CHEMBL3793310 (PubChem ID: 127030313), was negative to P-glycoprotein substrate (Pgp) interaction. In the case of Panobinostat, it had a high GI absorption, BBB permeability, and positive for Pgp substrate interaction, as given in table 4. The predicted pharmacokinetic properties of Cytochrome P450 for substrate and inhibition were also performed using the SwissADME online webserver. This included the CYP2D6 and CYP3A4 Substrate and CYP1A2, CYP2C19, CYP2D6 enzyme inhibition. The results show a high number of CYP450 interactions, given in **Table 4**.

The morden in silico modelling has played crucial roles in the early stages of the development of novel drugs, primarily in the ADME-Tox properties **[44]**. It has significantly reduced the cost, time and labour requirement that is necessary in the early stages of drug discovery **[44]**. The computational methods have enabled easier combination of various physicochemical properties of a molecule like solubility, pKa, oral bioavailability, volume of distribution, blood brain barrier permeability, skin permeability, metabolism and metabolic pathways, protein binding and clearance to accurately predict its pharmacokinetics **[44]**. Also these have shown usefulness in the potential toxicity predictions. Most of these predictions are based on the compound ADME data which were previously obtained through in vivo and in vitro studies.

The compiled data of molecular docking, binding energy, drug likeliness, pharmacokinetics including CYP450 interactions are used to compare Panobinostat with other molecules. This revealed that the top 5 molecules with the least binding energy show similar properties to Panobinostat. Molecules CHEMBL341601 (PubChem ID: 11058122), CHEMBL1819255 (Pubmed ID: 20579392), and 3-(4-(di(1H-indol-3-yl)methyl)phenyl)-N-hydroxyacrylamide (PubChem ID: 11993595) had no violations for the drug likeliness. The top molecules had high GI absorption and Pgp substrate interaction, while only CHEMBL341601 (PubChem ID: 11058122) had BBB permeability similar to Panobinostat. Similarly, the top molecules had CYP450 interaction as seen in Panobinostat. The low value of synthetic accessibility allows easier synthesis, where CHEMBL341601 (PubChem ID: 11058122) had the least value of 3.01 and was closest to Panobinostat at 2.88. These data imply that

they can be used as a potential target against the BCL6 gene.

The Brain Or Intestinal EstimateD permeation method (BOILED-Egg) was used for the visualization of the absorption pharmacokinetics of the top 5 molecules along with Panobinostat **(Figure 2)**. The plot suggested that only CHEMBL341601 (PubChem ID: 11058122) showed analogy to the absorption kinetics of Panobinostat in all the parameters of BBB permeation, Gastrointestinal absorption and PGP+. This along with this, the radar chart of CHEMBL341601 (PubChem ID: 11058122) and Panobinostat had similar bioavailability parameters **(Figure 3)**.

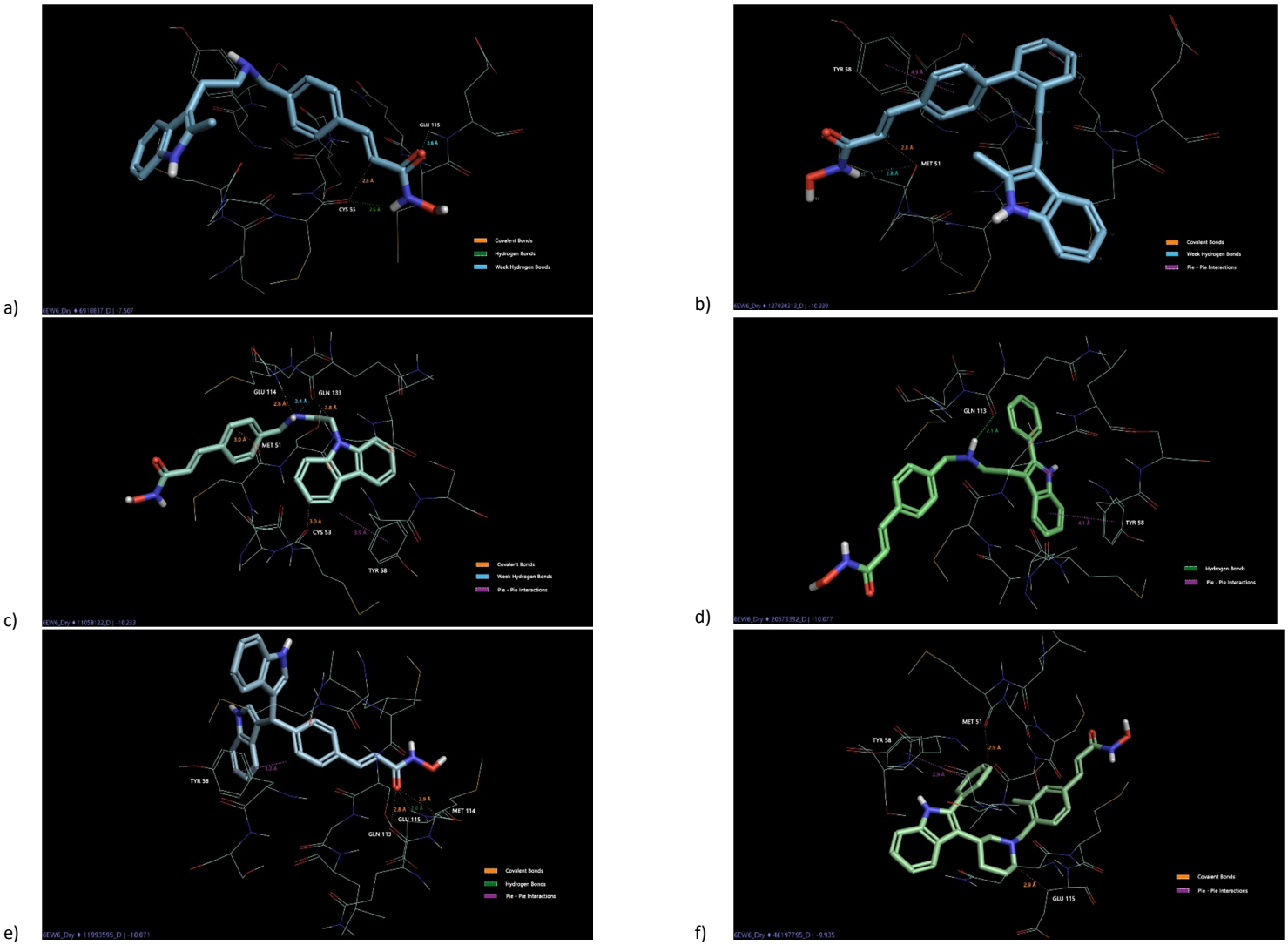

Figure 1: Molecular docking of a) Panobinostat, b) Molecule 1 CID127030313, c) Molecule 2 CID11058122, d) Molecule 3 CID20579392, e) Molecule 4 CID11993595 and f) Molecule 5 CID46197795 with BCL6 gene

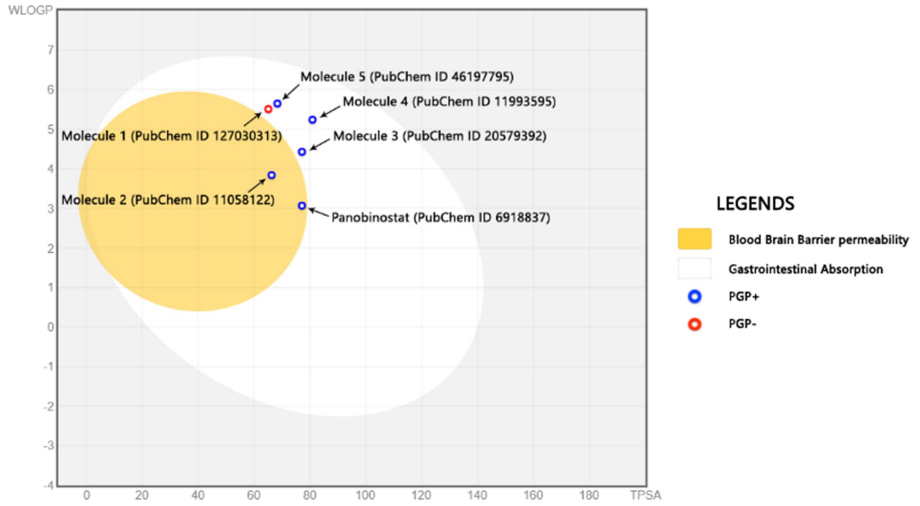

Figure 2: Predicted BOILED-Egg plot from swissADME online web tool of all molecules

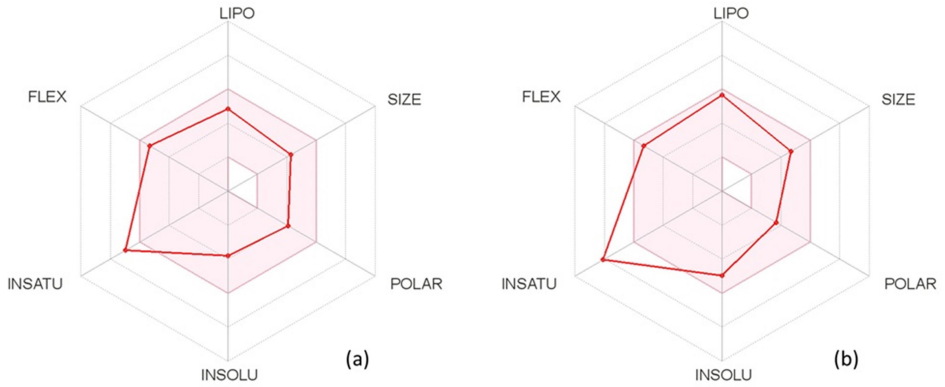

Figure 3: Bioavailability radar of (a) Panobinostat and (b) Molecule 2 CID11058122. The pink zone represents the space for oral bioavailability and red line indicates the oral bioavailability properties of the molecules.

Table 1: Drug Data of Panobinostat

Generic Drug Name	**Panobinostat**
Market Name	**Farydak (Pfizer)**
IUPAC Name	**(2E)-N-hydroxy-3-[4-({[2-(2-methyl-1H-indol-3-yl)ethyl]amino}methyl)phenyl]acrylamide**
Indication	**Marketed - Multiple myeloma** **Phase II/III - Chronic myeloid leukaemia** **Phase II - Acute myeloid leukaemia; Chronic lymphocytic leukaemia; Chronic myelomonocytic leukaemia; Colorectal cancer; Graft-versus-host disease; Lymphoma; Myelodysplastic syndromes; Myelofibrosis; Neuroendocrine tumours; Non-Hodgkin's lymphoma; Precursor cell lymphoblastic leukaemia-lymphoma; Renal cell carcinoma; Thyroid cancer; Waldenstrom's macroglobulinaemia** **Phase I/II - Breast cancer; HIV-1 infections; Hodgkin's disease; Malignant melanoma** **Phase I -Diffuse intrinsic pontine glioma**
Mechanism of Action	**Oral Histone Deacetylase Inhibitor**
Metabolism and Elimination	**Extensively metabolized, eliminated equally through the kidney and liver**
Primary Toxicities	**Thrombocytopenia, anemia, neutropenia, diarrhea, fatigue**

Table 2: Molecular interaction results of BCL6 with the top 5 molecules with the least binding energy

Compound (PubChem ID)	Interaction number	Interactions										Bond Length	Type of Bond
		Drug Molecule					Protein						
		Atom	Type	tf Value	Residue	Docked Score	Atom	Type	Name	tf Value	Residue		
127030313 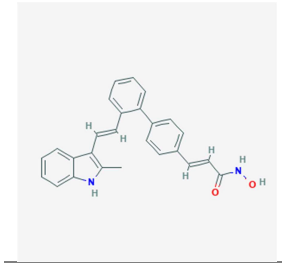	1	H 33	H	-0.175	Mol 1	-10.339	O 751	O sp2	O	13.84	A MET 51	2.8 Å	Hydrogen
	2	C 29	C sp2	-0.307	Mol 1	-10.339	O 751	O sp2	O	13.84	A MET 51	2.8 Å	Covalent
	3	C 16	C ar	-0.203	Mol 1	-10.339	C 848	C ar	CG	17.75	A TYR 58	4.9 Å	Pie – Pie
		C 21	C ar	-0.38	Mol 1	-10.339	C 849	C ar	CD1	18.57	A TYR 58		
		C 22	C ar	-0.134	Mol 1	-10.339	C 850	C ar	CD2	18.22	A TYR 58		
		C 26	C ar	-0.336	Mol 1	-10.339	C 851	C ar	CE1	20.01	A TYR 58		
		C 27	C ar	-0.155	Mol 1	-10.339	C 852	C ar	CE2	20.52	A TYR 58		
		C 25	C ar	-0.199	Mol 1	-10.339	C 853	C ar	CZ	25.97	A TYR 58		
11058122	1	C 24	C ar	-0.052	Mol 1	-10.233	O 778	O sp2	O	14.85	A CYS 53	3.0 Å	Covalent
	2	N 4	N sp3	-0.606	Mol 1	-10.233	N 1765	N tri	N	18.61	A GLU 114	2.8 Å	Covalent
	3	C 8	C sp3	-0.339	Mol 1	-10.233	O 1734	O sp2	O	14.6	A GLN 133	2.8 Å	Covalent
	4	H 31	H	-0.251	Mol 1	-10.233	O 1734	O sp2	O	14.6	A GLN 133	2.4 Å	Hydrogen

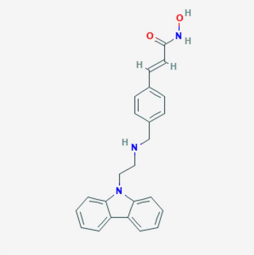	5	C 20	C ar	-0.287	Mol 1	-10.233	O 751	O sp2	O	13.84	A MET 51	3.0 Å	Covalent
	6	C 7	C ar	-0.247	Mol 1	-10.233	C 848	C ar	CG	17.15	A TYR 58	3.5 Å	Pie- Pie
		C 10	C ar	-0.218	Mol 1	-10.233	C 849	C ar	CD1	18.57	A TYR 58		
		C 13	C ar	-0.3	Mol 1	-10.233	C 850	C ar	CD2	18.22	A TYR 58		
		C 15	C ar	-0.307	Mol 1	-10.233	C 851	C ar	CE1	20.01	A TYR 58		
		C 18	C ar	-0.384	Mol 1	-10.233	C 852	C ar	CE2	20.521	A TYR 58		
		C 20	C ar	-0.287	Mol 1	-10.233	C 853	C ar	CZ	25.97	A TYR 58		
20579392 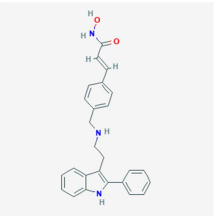	1	H 34	H	-0.505	Mol 1	-10.077	O 1734	O sp2	O	14.6	A GLN 113	2.1 Å	Hydrogen
	2	C 8	C ar	-0.182	Mol 1	-10.077	C 848	C ar	CG	17.15	A TYR 58	4.1 Å	Pie- Pie
		C 10	C ar	-0.136	Mol 1	-10.077	C 849	C ar	CD1	18.57	A TYR 58		
		C 13	C ar	-0.258	Mol 1	-10.077	C 850	C ar	CD2	18.22	A TYR 58		
		C 14	C ar	-0.181	Mol 1	-10.077	C 851	C ar	CE1	20.01	A TYR 58		
		C 16	C ar	-0.277	Mol 1	-10.077	C 852	C ar	CE2	20.521	A TYR 58		
		C 17	C ar	-0.218	Mol 1	-10.077	C 853	C ar	CZ	25.97	A TYR 58		
11993595 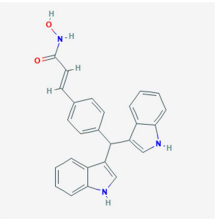	1	O 1	O sp2	-0.394	Mol 1	-10.071	H 1774	H	H	18.53	A GLU 115	2 Å	Hydrogen
	2	O 1	O sp2	-0.394	Mol 1	-10.071	C 1749	C sp3	CA	12.11	A MET 114	2.9 Å	Covalent
	3	O 1	O sp2	-0.394	Mol 1	-10.071	O 1734	O sp2	O	14.6	A GLN 113	2.8 Å	Covalent
	4	C 7	C ar	-0.132	Mol 1	-10.071	C 848	C ar	CG	17.15	A TYR 58	3.2 Å	Pie- Pie
		C 16	C ar	-0.318	Mol 1	-10.071	C 849	C ar	CD1	18.57	A TYR 58		
		C17	C ar	0.203	Mol 1	-10.071	C 850	C ar	CD2	18.22	A TYR 58		
		C 22	C ar	-0.39	Mol 1	-10.071	C 851	C ar	CE1	20.01	A TYR 58		
		C 23	C ar	-0.104	Mol 1	-10.071	C 852	C ar	CE2	20.521	A TYR 58		
		C 26	C ar	-0.255	Mol 1	-10.071	C 853	C ar	CZ	25.97	A TYR 58		
46197795	1	C 29	Car	-0.31	Mol 1	-9.935	O 715	O sp3	O	13.84	A MET 51	2.9 Å	Covalent
	2	C 11	C sp3	-0.238	Mol 1	-9.935	C 1769	C sp3	CB	23.03	A GLU 115	2.9 Å	Covalent
	3	C 18	C ar	-0.122	Mol 1	-9.935	C 848	C ar	CG	17.15	A TYR 58	5.0 Å	Pie- Pie
		C 25	C ar	-0.39	Mol 1	-9.935	C 849	C ar	CD1	18.57	A TYR 58		

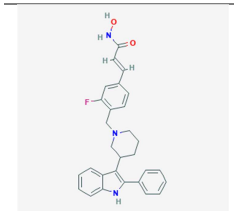		C 26	C ar	-0.175	Mol 1	-9.935	C 850	C ar	CD2	18.22	A TYR 58		
		C 29	C ar	-0.31	Mol 1	-9.935	C 851	C ar	CE1	20.01	A TYR 58		
		C 30	C ar	-0.175	Mol 1	-9.935	C 852	C ar	CE2	20.521	A TYR 58		
		C32	C ar	-0.021	Mol 1	-9.935	C 853	C ar	CZ	25.97	A TYR 58		
6918837 (Panobinostat) 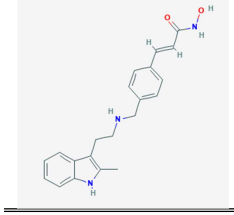	1	C 25	C sp2	-0.252	Mol 1	-7.507	O 778	O sp2	O	14.85	A CYS 53	2.8 Å	Covalent
	2	H 30	H	-0.297	Mol 1	-7.507	O 778	O sp2	O	14.85	A CYS 53	2.5 Å	Hydrogen
	3	O 1	O sp2	-0.527	Mol 1	-7.507	H 1774	H	H	18.53	A GLU 115	2.6 Å	Hydrogen

Table 3: Predicted drug likeliness and synthetic accessibility scores of the selected compounds

PubChem ID	Molecule	Lipinski violations	Ghose violations	Veber violations	Egan violations	Muegge violations	Synthetic Accessibility
127030313	Molecule 1	No	No	No	No	1 (XLOGP3>5)	3.45
11058122	Molecule 2	No	No	No	No	No	3.01
20579392	Molecule 3	No	No	No	No	No	3.31
11993595	Molecule 4	No	No	No	No	No	3.62
46197795	Molecule 5	No	2 (WLOGP>5.6, MR>130)	No	No	1 (XLOGP3>5)	4.14

Table 4: In-silico pharmacokinetic properties including GI absorption, BBB Permeability, P-glycoprotein substrate interaction and Cytochrome inhibition for the selected molecules

PubChem ID	Molecule	GI absorption	BBB permeant	Pgp substrate	CYP2D6 and CYP3A4 Substrate	CYP Enzymes Inhibition
127030313	Molecule 1	High	No	No	-	CYP1A2
11058122	Molecule 2	High	Yes	Yes	CYP2D6	CYP1A2, CYP2C19, CYP2D6
20579392	Molecule 3	High	No	Yes	CYP2D6 , CYP3A4	CYP1A2, CYP2C19
11993595	Molecule 4	High	No	Yes	CYP2D6	CYP2C9
46197795	Molecule 5	High	No	Yes	CYP2D6	CYP2C9

4. CONCLUSION

It can be concluded from the study and the collected data that CHEMBL341601 (PubChem ID: 11058122) was identified as the best ligand molecule with a high binding affinity for the BCL6 gene along with the optimal physicochemical properties for its ADME. These data imply that it can be used as a potential target against the BCL6 gene for the treatment of various types of cancer caused by alterations in the function of the BCL6 gene. Furthermore, the computational predicted data could be validated by in vitro and in vivo techniques using enzymatic assays and ADME analysis for future applications.

5. Acknowledgements

Declared none.

6. REFERENCES

[1] Global Cancer Observatory, "Non Hodgkin Lymphoma fact sheet," 2020. https://gco.iarc.fr/today/data/factsheets/cancers/34-Non-hodgkin-lymphoma-fact-sheet.pdf (accessed Oct. 02, 2021).

[2] E. N. Mugnaini and N. Ghosh, "Lymphoma.," *Prim. Care*, vol. 43, no. 4, pp. 661–675, Dec. 2016, doi: 10.1016/j.pop.2016.07.012.

[3] A. Jamil and S. K. R. Mukkamalla, *Lymphoma*. StatPearls Publishing, Treasure Island (FL), 2020.

[4] S. H. Swerdlow *et al.*, "The 2016 revision of the World Health Organization classification of lymphoid neoplasms.," *Blood*, vol. 127, no. 20, pp. 2375–2390, May 2016, doi: 10.1182/blood-2016-01-643569.

[5] J. W. Friedberg and R. I. Fisher, "Diffuse large B-cell lymphoma," *Hematol. Oncol. Clin. North Am.*, vol. 22, no. 5, pp. 941–ix, Oct. 2008, doi: 10.1016/j.hoc.2008.07.002.

[6] C. R. Flowers *et al.*, "Disparities in the early adoption of chemoimmunotherapy for diffuse large B-cell lymphoma in the United States.," *Cancer Epidemiol. biomarkers Prev. a Publ. Am. Assoc. Cancer Res. cosponsored by Am. Soc. Prev. Oncol.*, vol. 21, no. 9, pp. 1520–1530, Sep. 2012, doi: 10.1158/1055-9965.EPI-12-0466.

[7] S. A. Padala and A. Kallam, "Diffuse Large B Cell Lymphoma.," Treasure Island (FL), 2021.

[8] D. Allman *et al.*, "BCL-6 expression during B-cell activation.," *Blood*, vol. 87, no. 12, pp. 5257–5268, Jun. 1996.

[9] B. H. Ye *et al.*, "The BCL-6 proto-oncogene controls germinal-centre formation and Th2-type inflammation," *Nat. Genet.*, vol. 16, no. 2, pp. 161–170, 1997, doi:

10.1038/ng0697-161.

[10] B. H. Ye, "BCL-6 in the pathogenesis of non-Hodgkin's lymphoma.," *Cancer Invest.*, vol. 18, no. 4, pp. 356–365, 2000, doi: 10.3109/07357900009012179.

[11] S. M. Ranuncolo *et al.*, "Bcl-6 mediates the germinal center B cell phenotype and lymphomagenesis through transcriptional repression of the DNA-damage sensor ATR.," *Nat. Immunol.*, vol. 8, no. 7, pp. 705–714, Jul. 2007, doi: 10.1038/ni1478.

[12] W. Ci, J. M. Polo, and A. Melnick, "B-cell lymphoma 6 and the molecular pathogenesis of diffuse large B-cell lymphoma," *Curr. Opin. Hematol.*, vol. 15, no. 4, pp. 381–390, Jul. 2008, doi: 10.1097/MOH.0b013e328302c7df.

[13] R. T. Phan and R. Dalla-Favera, "The BCL6 proto-oncogene suppresses p53 expression in germinal-centre B cells.," *Nature*, vol. 432, no. 7017, pp. 635–639, Dec. 2004, doi: 10.1038/nature03147.

[14] S. M. Ranuncolo, J. M. Polo, and A. Melnick, "BCL6 represses CHEK1 and suppresses DNA damage pathways in normal and malignant B-cells.," *Blood Cells. Mol. Dis.*, vol. 41, no. 1, pp. 95–99, 2008, doi: 10.1016/j.bcmd.2008.02.003.

[15] R. T. Phan, M. Saito, K. Basso, H. Niu, and R. Dalla-Favera, "BCL6 interacts with the transcription factor Miz-1 to suppress the cyclin-dependent kinase inhibitor p21 and cell cycle arrest in germinal center B cells.," *Nat. Immunol.*, vol. 6, no. 10, pp. 1054–1060, Oct. 2005, doi: 10.1038/ni1245.

[16] Gene Cards, "BCL6 Gene - BCL6 Transcription Repressor." https://www.genecards.org/cgi-bin/carddisp.pl?gene=BCL6 (accessed Oct. 04, 2021).

[17] P. W. M. Johnson and A. J. Davies, "Primary mediastinal B-cell lymphoma.," *Hematol. Am. Soc. Hematol. Educ. Progr.*, pp. 349–358, 2008, doi: 10.1182/asheducation-2008.1.349.

[18] F. Leithäuser, M. Bäuerle, M. Q. Huynh, and P. Möller, "Isotype-switched immunoglobulin genes with a high load of somatic hypermutation and lack of ongoing mutational activity are prevalent in mediastinal B-cell lymphoma.," *Blood*, vol. 98, no. 9, pp. 2762–2770, Nov. 2001, doi: 10.1182/blood.v98.9.2762.

[19] A. Rosenwald *et al.*, "Molecular diagnosis of primary mediastinal B cell lymphoma identifies a clinically

favorable subgroup of diffuse large B cell lymphoma related to Hodgkin lymphoma.," *J. Exp. Med.*, vol. 198, no. 6, pp. 851–862, Sep. 2003, doi: 10.1084/jem.20031074.

[20] K. J. Savage *et al.*, "The molecular signature of mediastinal large B-cell lymphoma differs from that of other diffuse large B-cell lymphomas and shares features with classical Hodgkin lymphoma.," *Blood*, vol. 102, no. 12, pp. 3871–3879, Dec. 2003, doi: 10.1182/blood-2003-06-1841.

[21] "FDA Approves Panobinostat for Some Patients with Multiple Myeloma," *National Cancer Institute*, 2015. https://www.cancer.gov/news-events/cancer-currents-blog/2015/fda-approves-panobinostat (accessed Oct. 14, 2021).

[22] "LiverTox: Clinical and Research Information on Drug-Induced Liver Injury," *Bethesda (MD): National Institute of Diabetes and Digestive and Kidney Diseases*, 2020. https://www.ncbi.nlm.nih.gov/books/NBK548331/ (accessed Oct. 11, 2021).

[23] K. Tzogani *et al.*, "EMA Review of Panobinostat (Farydak) for the Treatment of Adult Patients with Relapsed and/or Refractory Multiple Myeloma.," *Oncologist*, vol. 23, no. 5, pp. 631–636, May 2018, doi: 10.1634/theoncologist.2017-0301.

[24] P. D. Gregory, K. Wagner, and W. Hörz, "Histone acetylation and chromatin remodeling.," *Exp. Cell Res.*, vol. 265, no. 2, pp. 195–202, May 2001, doi: 10.1006/excr.2001.5187.

[25] P. Marks, R. A. Rifkind, V. M. Richon, R. Breslow, T. Miller, and W. K. Kelly, "Histone deacetylases and cancer: causes and therapies.," *Nat. Rev. Cancer*, vol. 1, no. 3, pp. 194–202, Dec. 2001, doi: 10.1038/35106079.

[26] S. Ropero and M. Esteller, "The role of histone deacetylases (HDACs) in human cancer.," *Mol. Oncol.*, vol. 1, no. 1, pp. 19–25, Jun. 2007, doi: 10.1016/j.molonc.2007.01.001.

[27] A. A. Lane and B. A. Chabner, "Histone deacetylase inhibitors in cancer therapy.," *J. Clin. Oncol. Off. J. Am. Soc. Clin. Oncol.*, vol. 27, no. 32, pp. 5459–5468, Nov. 2009, doi: 10.1200/JCO.2009.22.1291.

[28] E. Eleutherakis-Papaiakovou, N. Kanellias, E. Kastritis, M. Gavriatopoulou, E. Terpos, and M. A. Dimopoulos, "Efficacy of Panobinostat for the Treatment of Multiple Myeloma," *J. Oncol.*, vol.

2020, p. 7131802, 2020, doi: 10.1155/2020/7131802.

[29] M. Van Veggel, E. Westerman, and P. Hamberg, "Clinical Pharmacokinetics and Pharmacodynamics of Panobinostat," *Clin. Pharmacokinet.*, vol. 57, no. 1, pp. 21–29, 2018, doi: 10.1007/s40262-017-0565-x.

[30] S. E. Assouline *et al.*, "Phase 2 study of panobinostat with or without rituximab in relapsed diffuse large B-cell lymphoma.," *Blood*, vol. 128, no. 2, pp. 185–194, Jul. 2016, doi: 10.1182/blood-2016-02-699520.

[31] W. W. Tan *et al.*, "Phase I Study of Panobinostat (LBH589) and Letrozole in Postmenopausal Metastatic Breast Cancer Patients.," *Clin. Breast Cancer*, vol. 16, no. 2, pp. 82–86, Apr. 2016, doi: 10.1016/j.clbc.2015.11.003.

[32] H. S. Takhar, N. Singhal, R. Gowda, M. Penniment, P. Takhar, and M. P. Brown, "Phase I study evaluating the safety and efficacy of oral panobinostat in combination with radiotherapy or chemoradiotherapy in patients with inoperable stage III non-small-cell lung cancer.," *Anticancer. Drugs*, vol. 26, no. 10, pp. 1069–1077, Nov. 2015, doi: 10.1097/CAD.0000000000000282.

[33] J. E. Gray *et al.*, "A phase I, pharmacokinetic, and pharmacodynamic study of panobinostat, an HDAC inhibitor, combined with erlotinib in patients with advanced aerodigestive tract tumors.," *Clin. cancer Res. an Off. J. Am. Assoc. Cancer Res.*, vol. 20, no. 6, pp. 1644–1655, Mar. 2014, doi: 10.1158/1078-0432.CCR-13-2235.

[34] H. M. Berman *et al.*, "The Protein Data Bank," *Nucleic Acids Res.*, vol. 28, no. 1, pp. 235–242, Jan. 2000, doi: 10.1093/nar/28.1.235.

[35] J. A. Amaya, D. Batabyal, and T. L. Poulos, "Proton Relay Network in the Bacterial P450s: CYP101A1 and CYP101D1," *Biochemistry*, vol. 59, no. 31, pp. 2896–2902, Aug. 2020, doi: 10.1021/acs.biochem.0c00329.

[36] T. Cheeseright, M. Mackey, S. Rose, and A. Vinter, "Molecular Field Extrema as Descriptors of Biological Activity: Definition and Validation," *J. Chem. Inf. Model.*, vol. 46, no. 2, pp. 665–676, Mar. 2006, doi: 10.1021/ci050357s.

[37] Bethesda (MD): National Library of Medicine (US), "PubChem Compound Summary for CID 6918837, Panobinostat.," *National Center for Biotechnology Information.*, 2021. https://pubchem.ncbi.nlm.nih.gov/co

mpound/Panobinostat. (accessed Oct. 15, 2021).

[38] M. R. Bauer and M. D. Mackey, "Electrostatic Complementarity as a Fast and Effective Tool to Optimize Binding and Selectivity of Protein–Ligand Complexes," *J. Med. Chem.*, vol. 62, no. 6, pp. 3036–3050, Mar. 2019, doi: 10.1021/acs.jmedchem.8b01925.

[39] C. A. Lipinski, F. Lombardo, B. W. Dominy, and P. J. Feeney, "Experimental and computational approaches to estimate solubility and permeability in drug discovery and development settings.," *Adv. Drug Deliv. Rev.*, vol. 46, no. 1–3, pp. 3–26, Mar. 2001, doi: 10.1016/s0169-409x(00)00129-0.

[40] W. J. Egan, Merz Kenneth M., and J. J. Baldwin, "Prediction of Drug Absorption Using Multivariate Statistics," *J. Med. Chem.*, vol. 43, no. 21, pp. 3867–3877, Oct. 2000, doi: 10.1021/jm000292e.

[41] I. Muegge, "Pharmacophore Features of Potential Drugs," *Chem. – A Eur. J.*, vol. 8, no. 9, pp. 1976–1981, May 2002, doi: https://doi.org/10.1002/1521-3765(20020503)8:9<1976::AID-CHEM1976>3.0.CO;2-K.

[42] A. K. Ghose, V. N. Viswanadhan, and J. J. Wendoloski, "A knowledge-based approach in designing combinatorial or medicinal chemistry libraries for drug discovery. 1. A qualitative and quantitative characterization of known drug databases.," *J. Comb. Chem.*, vol. 1, no. 1, pp. 55–68, Jan. 1999, doi: 10.1021/cc9800071.

[43] D. F. Veber, S. R. Johnson, H.-Y. Cheng, B. R. Smith, K. W. Ward, and K. D. Kopple, "Molecular properties that influence the oral bioavailability of drug candidates.," *J. Med. Chem.*, vol. 45, no. 12, pp. 2615–2623, Jun. 2002, doi: 10.1021/jm020017n.

[44] J. Ghosh, M. S. Lawless, M. Waldman, V. Gombar, and R. Fraczkiewicz, "Modeling ADMET.," *Methods Mol. Biol.*, vol. 1425, pp. 63–83, 2016, doi: 10.1007/978-1-4939-3609-0_4.